More rapid intensification of flash droughts with shorter onset timescales

Yamin Qing
Hong Kong Polytechnic University
Shuo Wang (shuo.s.wang@polyu.edu.hk)
Hong Kong Polytechnic University https://orcid.org/0000-0001-7827-187X
Brian C. Ancell
Texas Tech University
Zong-Liang Yang
University of Texas at Austin https://orcid.org/0000-0003-3030-0330

Article

Keywords: Onset Development Phase, Regional Humidity, Intensification Rate, Flash Drought Evolution Acceleration, Drought Monitoring Systems

Posted Date: March 10th, 2021

DOI: https://doi.org/10.21203/rs.3.rs-267288/v1

Version of Record: A version of this preprint was published at Nature Communications on March 3rd, 2022. See the published version at https://doi.org/10.1038/s41467-022-28752-4.

More rapid intensification of flash droughts with shorter onset timescales

Y. Qing[1], S. Wang[1,2,*], B. C. Ancell[3], and Z. L. Yang[4]

1. Department of Land Surveying and Geo-Informatics, The Hong Kong Polytechnic University, Hong Kong, China
2. The Hong Kong Polytechnic University Shenzhen Research Institute, Shenzhen, China
3. Department of Geosciences, Texas Tech University, Lubbock, TX, USA
4. Department of Geological Sciences, The John A. and Katherine G. Jackson School of Geosciences, University of Texas at Austin, Austin, TX, USA

*Corresponding author: Shuo Wang (shuo.s.wang@polyu.edu.hk)

Abstract

Flash droughts can cause more serious environmental and agricultural impacts than traditional droughts because of the sudden onset and rapid intensification. However, it remains unclear how rapidly flash droughts develop and intensify worldwide. Here, we present for the first time a comprehensive assessment of the onset development phase of flash droughts on a global scale. We find that humid and semi-humid regions are more vulnerable to flash droughts. And 56.8% of flash droughts are extremely fast-developing (timescale $\leq$ 15 days) and intensifying (intensification rate $\geq$ 12.5th percentile) droughts during 2000–2019. More importantly, the evolution of flash droughts is accelerating with a significantly shorter timescale and a faster intensification, implying that less time is left for early warning and impact preparation. Our findings suggest that urgent action is needed to upgrade existing drought monitoring systems for better capturing the more rapid onset and evolution of flash droughts.

1. Introduction

Flash droughts, as a new drought type, have been receiving increasing attention from the scientific community in recent years. Compared with traditional, more slowly developing droughts, flash droughts evolve with a rapid onset development along with a fast depletion of water availability that may cause an imbalance of ecosystems and agricultural systems (Otkin et al., 2015a; Crausbay et al., 2017). Since flash droughts can be distinguished by their rapid development, there is no early warning for impact preparation, potentially causing more severe impacts on agriculture and society than the slowly-evolving droughts (Svoboda et al., 2002; Otkin et al., 2018). For example, a historical flash drought that occurred over the Central United States without early warning caused a tremendous impact on agricultural production and the economy, with $12 billion losses attributed to this event (Hoerling et al., 2014). The flash drought event that occurred over Southern Queensland, Australia in 2018 de-vegetated the landscape and drove livestock numbers to the lowest level in the country (Nguyen et al., 2019). Under the influence of global warming, flash droughts have occurred more frequently in recent years, including those in southern China (Wang et al., 2016; Wang and Yuan, 2018; Yuan et al., 2019b), USA (Hoerling et al., 2014; Gerken et al., 2018), and Africa (Yuan et al., 2018). In addition, heat waves may also manifest during flash droughts, which can further lead to significant impacts on agricultural yields and loss of life (Thacker et al., 2008; Mo and Lettenmaier, 2015).

There is currently a lack of a consistent definition of flash droughts. The definitions proposed in previous studies can be generally classified into two types. One is based on the duration of flash droughts. And the widely used definition was proposed by Mo and Lettenmaier (2015, 2016), which used different combinations of thresholds of soil moisture, temperature, precipitation, and evapotranspiration to identify flash drought events. Another is based on the rapid intensification rate of flash droughts (Ford, 2017; Otkin et al., 2018; Liu et al., 2020; Yuan et al., 2020). These two types of definitions of flash droughts provide us with alternative approaches to access this extreme phenomenon from different perspectives (duration and intensification rate). On the other hand, there are a variety of indices available to identify flash droughts, including the Evaporative Demand Drought Index (EDDI) (Hobbins et al., 2016; Mcevoy et al., 2016), the Evaporative Stress Index (ESI) (Anderson et al., 2016; Otkin et al., 2016; Nguyen et al., 2019), the Standard Evaporative Stress Ratio (SESR) (Basara et al., 2019), the combination of the ESI and the Rapid Change Rate Index (RCI) (Anderson et al., 2013; Otkin et al., 2014; Otkin et al., 2015b), precipitation (Hunt et al., 2014), vegetation (Sun et al., 2015), and soil moisture (Ford et al., 2017; Liu et al., 2019; Yuan et al., 2019b; Liu et al., 2020; Mahto et al., 2020). Moreover, several definitions were proposed based on the US Drought Monitor (USDM) (Ford et al., 2015; Lorenz et al., 2018; Pendergrass et al., 2020). Previous studies have indicated that soil moisture anomalies are useful for characterizing the drought onset, particularly for rapid onset droughts (Hunt et al., 2009; Mozny et al., 2012). The rapid decrease in soil moisture could potentially serve as a precursor for flash droughts (Otkin et al., 2017). Moreover, Osman et al. (2021) examined the key climate variables used in flash drought definitions, including precipitation, root zone soil moisture, temperature, and actual and potential evapotranspiration. And they found that the root zone soil moisture shows the clearest signal when flash droughts occur.

The occurrence of flash droughts has been examined in many regions worldwide, but most studies are limited to a basin (Li et al., 2020; Liu et al., 2020), several states (Ford et al., 2015; Ford et al., 2017; Gerken et al., 2018; Basara et al., 2019), or a country (Mo and Lettenmaier et

al., 2015; Otkin et al., 2015a; Christian et al., 2019; Nguyen et al., 2019; Yuan et al., 2019b; Mahto et al., 2020). There is a lack of global assessment of flash droughts. In addition, the effects of climate change vary from region to region, and thus have important implications for extremes, such as droughts and floods (Sivakumar et al., 2011b; Yang and Yang, 2012). Further, local and regional extreme events are conditioned by large-scale atmospheric circulation that can drive extremes to vary across different regions under potential processes including upper-level ridges, land-atmospheric interactions, and monsoons (Waliser et al., 2003; Hendon et al., 2007; Pendergrass et al., 2020). These processes influence the climate characteristics and the occurrence of flash droughts over different regions around the world. Thus, a global picture of flash droughts is desired to reveal the spatial pattern and temporal variability of flash droughts, advancing our understanding of flash droughts on a global scale.

Flash droughts can be viewed as a subset of droughts that are distinguished from slowly developing droughts by their rapid onset development (Otkin et al., 2017). The rapid onset development must include not only a rapid onset but also a rapid rate of intensification. The rapid onset is a turning point, which depicts a shift from non-drought to drought conditions, but it lacks an interpretation of the process of change. The rapid intensification rate can characterize either the onset or the later phase of drought events, and thus it can depict a developed drought becoming more severe but cannot represent the beginning of a flash drought event. Even though it is recognized that flash droughts evolve rapidly during the onset development (Ford et al., 2017; Otkin et al., 2018; Yuan et al., 2018; Basara et al., 2019), it remains unclear that how fast flash droughts evolve. Does the rapid development take place within one week, one month, or longer time? On the other hand, the rapid development must be accompanied by high intensification. Is the onset development of flash droughts intensifying? Exploring the onset development timescales and the intensification of flash droughts can provide insights into the prediction of flash droughts and the development of early warning systems for mitigating the impacts of flash droughts.

Here, we explore the rapid onset development of flash droughts identified by taking into account both flash (a rapid onset accompanied by a rapid intensification rate) and drought severity (soil moisture drops below a specific threshold for a period of time) on a global scale. Specifically, we examine spatial patterns of flash droughts and reveal how fast flash droughts develop over the past 20 years from 2000 to 2019. This is the first global study to identify hot spots of flash droughts and to shed light on the onset development timescales and intensification of flash droughts, advancing our understanding of the evolution tendency of flash droughts and providing insights into the implementation of flash drought forecasts and early warning systems.

2. Results and Discussion

2.1 Identification of global hot spots of flash droughts and underlying mechanisms

We compared the global patterns of flash droughts identified by two different definitions based on the intensification rate and the duration of flash droughts, respectively. Fig. 1a, b show the variations in soil moisture percentiles for flash drought events of all grid points, identified by the intensification rate (Fig. 1a) and the duration (Fig. 1b) of flash droughts. To satisfy the drought condition, soil moisture should decrease to a critical level (the 20th percentile threshold) because soil moisture below such a threshold indicates a start of abnormally dry conditions that have a large impact on the environment (Svoboda et al., 2002). As shown in Fig. 1a, all events reach

below the 20th percentile after a rapid decline in soil moisture. By contrast, 13−37% of the events detected by the old definition (from the perspective on duration) (Fig. 1b) would be viewed as non-drought events since soil moisture only decreases from above the 40th percentile to above the 30th percentile. Further, 24−59% of the detected events could be classified as non-moderate drought events since soil moisture just declines to over the 20th percentile (according to the thresholds to classify the severity of drought events used by the U.S. Drought Monitor). As for another feature (flash), a rapid decline in soil moisture should be characterized to identify flash droughts. The events captured based on the new definition present a sharp decrease in soil moisture from above the 40th percentile to below the 20th percentile within one month, and soil moisture below the 20th percentile lasts for no less than 2 pentads. In comparison, only 11−31% of the events identified by the old definition experience a rapid decline (soil moisture decreases from the 40th percentile to the 20th percentile) in soil moisture over the period of the onset development phase (Fig. 1b). In addition, 16−49% of the events with soil moisture decreasing to below the 40th percentile occur, but then rapidly recover up to the 40th percentile within only a pentad under abnormal dry conditions. These events cannot be viewed as flash droughts because only one pentad is insufficient to diminish crop productivity and yield. Therefore, the use of the definition focusing solely on the duration of flash droughts cannot guarantee that all events satisfy the key characteristics (flash and drought severity) of flash droughts.

The frequencies of flash droughts identified by the new definition are lower than those detected by the old definition (Fig. 1c-f). This is because the use of the old definition captures more events that last for only one pentad. Nonetheless, both methods (definitions) indicate that flash droughts are mostly likely to occur in humid and semi-humid regions (e.g., North Asia, East Asia, Southeast Asia, Eastern North America, and Central North America), but less in water-limited areas (e.g., South Asia, Western Africa, Eastern Africa, Southern Africa, and Australia). This is consistent with previous studies (Wang et al., 2016; Ford and Labosier, 2017; Zhang et al., 2017; Yuan et al., 2019). Particularly, the hot spots for the high frequency of flash droughts are highlighted, and the contributions to the high frequency of flash droughts are related to different phenomena of atmospheric circulation. As East Asia and Southeast Asia (red boxes in Fig. 1c) are tropical monsoon climate regions (Lau et al., 1997; Wen et al., 2016), the break of monsoons plays an important role in triggering the high frequency of flash droughts. During the break of monsoons, the prolonged significant negative anomaly of precipitation may lead to a rise in temperature, which in turn causes a rapid depletion in soil moisture. Furthermore, the combination of significant negative precipitation and positive temperature anomalies could lead to an increased atmospheric water demand that accelerates the decline in soil moisture (Zhang et al., 1996; Huang et al., 2007; Zhang et al., 2013; Yuan et al., 2019; Mahto and Mishra, 2020). For the hot spots in Central North America and Eastern North America, the predominant factor may be the upper-level ridge (yellow boxes in Fig. 1c). The ridge brings widespread unusual warm temperatures and, by itself, would have been responsible for dry conditions as well. Meanwhile, the ridge may inhibit precipitation over the regions missed by the upper-level trough, with precipitation deficit occurring over these regions, which may cause abnormal dryness expanded and intensified or even the occurrence of flash drought events (Namias, 1983; Schubert et al., 2009; Burrows et al., 2019; Christian et al., 2020). In addition, land–atmosphere coupling also plays a crucial role in driving the occurrence of flash droughts (green boxes in Fig. 1c), which influences the diurnal precipitation cycle through the surface heat and moisture fluxes. The enhanced signal for land-atmosphere coupling could amplify temperature extremes and thus a rapid decline in soil moisture, which creates a favorable

environment for the occurrence of flash droughts (Fischer et al., 2007; Kumar et al., 2011; Soares et al., 2019).

2.2 Assessment of onset development timescales and intensification rates of flash droughts

To facilitate further understanding of flash drought characteristics, we divided the whole world into 21 regions for conducting an in-depth regional analysis of flash droughts (Supplementary Table 1). Among them, Greenland, Alaska, and Sahara are excluded from our analyses because there are no agricultural activities there. To conduct a comprehensive assessment of the lead time of flash droughts around the world, we divided flash droughts into five different types according to the longest possible onset development phase of flash droughts (≤ 1 month was proposed by Otkin et al. (2017)), including 1 pentad, 2 pentads, 3 pentads, 4 pentads, and 5 pentads. Fig. 2 compares the percentages of flash droughts at different lead times among all flash droughts as well as their mean intensification rates. In general, 56.8% of flash droughts developed in less than or equal to 3 pentads, especially in Southeast Asia, East Asia, Tibet, and Central North America where the proportion of flash droughts developing in less than or equal to 3 pentads is up to 65.2% (Supplementary Fig. 1 and Fig. 2). Furthermore, 2.2% and 9.8% of flash droughts occurred in 1 and 2 pentads, with a mean intensification rate of the 28.6th percentile and the 16.4th percentile, respectively. Specifically, over 32.1% of flash droughts occurred in 2 pentads over Southeast Asia and East Asia. In comparison, there are 28.8% and 14.4% of flash droughts developing in 4 and 5 pentads, respectively. And the mean intensification rates of flash droughts at 4- and 5-pentad lead times are the 11.6th and 11.3th percentiles, respectively. Thus, flash droughts developed much faster than traditional droughts, with more than half of flash droughts developing within half a month (≤ 3 pentads). Such an unusual intensification rate may be triggered by extremes of multiple factors (e.g., extreme high temperature and precipitation deficit). For example, Queensland experienced the extreme high temperature coinciding with an extreme deficit of precipitation in January 2018, which caused a flash drought event that lasted from January to June in 2018 (Nguyen et al., 2019). In addition, vegetation is another main reason for the rapid onset development of flash droughts because of its important role in mediating the transpiration. Crops can be moisture-stress much more quickly by pumping water from deep soil, which may trigger a rapid development of flash droughts (see the global cropland distribution in Supplementary Fig. 3, the distribution of intensive crop production areas is consistent with a large part of intensive flash drought areas). As the rapid onset poses a huge challenge for drought monitoring, assessing the relatively fast onset development timescales of flash droughts can provide useful information for upgrading drought monitoring systems. Specifically, the existing drought monitoring systems are updated at a monthly or weekly timescale. Given the rapid onset timescales of more than 50% of flash droughts developing in less than or equal to 3 pentads and even several flash droughts occurring within 5 days, existing drought monitoring systems are incapable of catching flash droughts.

We used the nonparametric Mann-Kendall statistic to examine the changes in the percentages of flash droughts at different lead times among all flash drought events at an annual timescale. The number of flash droughts developing in 1 and 2 pentads is too small to perform statistical significance tests within a 20-year period, and thus we incorporated the events at 1-, 2-, and 3-pentad lead times into one category (≤ 3 pentads). Fig. 3a-c show the spatial patterns of the Mann-Kendall trends for flash droughts developing in less than or equal to 3 pentads as well as 4 and 5 pentads over the period of 2000−2019. In general, the frequency of flash drought events at

less than or equal to 3-pentad lead times is increasing on a global scale, with the areas showing an upward trend of 32.7% and the areas showing a downwards trend of 18.7% (Fig. 3d). Over most regions, the areas with an upward trend are larger than those with a downward trend (Supplementary Fig. 4), indicating that the onset of flash droughts is becoming much faster over these regions. By contrast, flash drought events at 4- and 5-pentad lead times show that the areas with a downward trend are larger than those with an upward trend (Fig. 3e, f). In addition, the flash droughts developing in less than or equal to 3 pentads show a statistically significant ($p < 0.01$) increase from 56.3% in 2000 to 69.8% in 2019, implying that flash droughts have been becoming faster (Fig. 4a). Similar trends can also be found in most sub-regions, with the highest increasing trend over East Asia, followed by Central North America, Eastern North America, and Southeast Asia (Supplementary Fig. 5). By contrast, flash drought events at 4- and 5-pentad lead times indicate a downward trend globally, which show a statistically significant ($p < 0.01$) decrease from 28.3% and 13.3% in 2000 to 23.2% and 9.3% in 2019 (Fig. 4b, c). As the flash drought evolves faster, the mean intensification rate of onset development also shows a significant ($p < 0.05$) increase from the 13.2th percentile in 2000 to the 14.4th percentile in 2019 (Fig. 4d). Therefore, flash droughts are becoming faster and intensifying over the period of 2000−2019.

Faster developing flash droughts are attributed to faster soil moisture changes under the influence of relevant climate factors. In fact, a rapid decline in soil moisture is not only because of a lack of rain; it is also affected by high temperature. For example, a strong wind can lead to a rapid decline in soil moisture on a hot and dry day. Flash droughts occur when soil moisture reaches an abnormally dry condition. Particularly, these dry periods could worsen while coinciding with growing seasons, such as the case in the US Midwest's 2012 flash drought event (Basara et al., 2019; Jin et al., 2019). In addition, landscape can dry out quickly under global warming even after a wet winter and spring since the warmer climate accelerates the hydrological cycle. On the other hand, a general increase in air temperature can lead to an increase in soil temperature. Warmer soil temperature accelerates soil processes, such as enhancing the transpiration rate, and thus plants tend to acquire water more readily as temperature increases (Rajib et al., 2016). As a consequence, these could be the potential reasons for the faster development of flash droughts.

We compared the occurrence of flash droughts and all drought events when soil moisture reached a threshold of the 20th percentile, regardless of whether or not they showed a rapid onset. There is remarkably contrasting and high spatial variability in the percentages of flash droughts among all droughts globally (Fig. 4f). The relatively high percentages of flash droughts among all drought events are found over the humid and semi-humid regions (Supplementary Fig. 6). And the percentages of flash droughts among all droughts show a statistically significant ($p < 0.05$) upward trend over the entire period, with an increase from 11.3% in 2000 to 14.1% in 2019 globally (Fig. 4e). Specifically, there is a remarkably increasing trend in the percentages of flash droughts among all droughts over most regions, including South Asia, Southern South America, Eastern North America, Western North America, Western Africa, and Eastern Africa (Supplementary Fig. 7). The increase in the number of flash droughts accompanied by the faster and intensifying onset development phase indicates that more droughts take less time to develop, thereby posing a great challenge for drought detection and prediction at relatively short timescales. Consequently, urgent action is needed to develop flash drought prediction tools and early warning systems for better capturing key characteristics of flash droughts.

2.3 Effects of soil moisture thresholds and soil layers on the identification of flash droughts

It should be noted that the frequency of flash droughts is largely affected by the thresholds of soil moisture chosen to identify flash droughts. We compared the frequencies of occurrence of flash droughts under different percentile thresholds of soil moisture (Supplementary Fig. 8). We find that the spatial patterns are similar under different thresholds, but the number of detected flash droughts varies greatly. When lifting the soil moisture percentile to the 50th percentile, the number of detected flash droughts is too small to carry out tests for statistical significance over most regions of the world for the period of 2000−2019. More flash drought events can be identified when the threshold decreases to the 30th percentile, but such a decline in soil moisture from the 30th to the 20th percentile may not capture the flash condition (rapid intensification of a drought condition). For example, when soil moisture decreases from the 30th percentile to the 20th percentile within one month, the average intensification rate of each pentad is only the 2th percentile that is too low to consider as a rapid intensification. The threshold of the 40th percentile was thus used in this study.

We also conducted sensitivity tests by changing soil depths. By comparing flash drought frequencies identified by soil moisture in the top and the root zone layers (Supplementary Fig. 9), we find that the difference in flash drought frequencies derived based on different soil depths is larger than the resulting difference using different soil moisture thresholds. The use of top-layer soil moisture is able to capture more flash drought events since the top-layer soil responds quickly to the evapotranspiration increase and the precipitation deficit. In comparison, the water stored in the root zone layer is directly available to support plant growth, which is a dominant factor in agricultural productivity. The deficit in the root-zone soil moisture can result in plant death and yield loss. Thus, we identified flash droughts based on the changes in the root-zone soil moisture instead of the top-layer soil moisture.

2.4 Sensitivities of soil moisture to variations in precipitation and evapotranspiration

It is widely accepted that the rapid intensification rate of flash droughts is caused by moisture imbalance that is related to precipitation and evapotranspiration (Pendergrass et al., 2020). The increase (decrease) in precipitation can lead to the corresponding increase (decrease) in soil moisture. The increase (decrease) in evapotranspiration also contributes to the decrease (increase) in soil moisture. Thus, precipitation and evapotranspiration are the key factors that trigger flash droughts. Nonetheless, soil moisture across different regions shows different sensitivities to the variations in precipitation and evapotranspiration, which poses a great challenge of investigating flash droughts globally.

Previous studies have indicated that the soil moisture variability in arid regions is too weak to cause strong evapotranspiration responses (Koster et al., 2009; Mo and Lettenmaier 2016). Thus, precipitation plays an important role in triggering flash droughts in dry regions. This is the reason why in the precipitation-deficit regions (Southern South America, Western Africa, Southern Africa, and Eastern Africa), the frequency of flash droughts is low in our study. On the other hand, soil moisture in arid regions is relatively low, and thus it is difficult to experience a considerable decrease to capture the key feature of flash droughts (greater than the 5th percentile intensification rate in soil moisture). This is the reason why there is a relatively small number of flash droughts captured by our method. Arid regions are favorable to traditional droughts, but flash droughts occur less often over these regions (Supplementary Fig. 10). Therefore, our method using the

changes in soil moisture may show poor performance in capturing flash droughts driven by the precipitation deficit.

3. Conclusions

For the first time, we examined the global patterns of flash droughts and underlying mechanisms based on a new definition. We explored the onset development timescales of flash droughts on a global scale and revealed how rapidly flash droughts have been intensifying in a changing environment. Our findings disclose that flash droughts tend to occur in humid and semi-humid regions, including North Asia, East Asia, Southeast Asia, Eastern North America, and Central North America. And the onset development of flash droughts is becoming faster, with 56.8% of flash droughts developing in less than or equal to 3 pentads for the period of 2000−2019. Specifically, the frequencies of flash droughts at less than or equal to 3-pentad lead times are increasing significantly, with a mean intensification rate of more than the 13.2th percentile, whereas flash drought events at 4- and 5-pentad lead times show an evident decrease globally. In addition, the percentage of flash droughts among all drought events shows an upward trend globally. The identification of flash drought-prone regions and global hot spots can provide valuable insights to help inform policymakers and stakeholders on potential risks of flash droughts that have a large impact on plant growth and crop yield. The recent increase in the frequency and intensification of extremely fast-developing flash droughts suggests that urgent action is needed to upgrade existing drought prediction and early warning systems for better capturing the more rapid onset and evolution of flash droughts.

4. Methods

4.1 Datasets

We used the surface air temperature (T), precipitation (P), evapotranspiration (ET), and soil moisture (SM), derived from three NASA GLDAS-2 (Global Land Data Assimilation System Version 2) models (Xia et al., 2012a, b) including VIC (Liang et al., 1996), Noah (Ek et al., 2003; Barlage et al., 2010; Wei et al., 2013), and Catchment land surface models (Rienecker et al., 2008, 2011) with a spatial resolution of 1.0 degree and a temporal resolution of three hours for 2000−2019 (Rodell et al., 2004). GLDAS has been proven to be able to reflect global and regional trends and patterns in SM (Dorigo et al., 2012; Jia et al., 2018). Due to the good performance of GLDAS, it has been widely used to analyze global and regional SM changes (Zawadzki and Kedzior, 2014; Cheng et al., 20). Specifically, the root zone SM, derived from each land surface model, was used to identify flash droughts since the rapid decline in SM can serve as a precursor for flash droughts, particularly if the plant-available soil moisture approaches the wilting point (Otkin et al., 2017).

First, we calculated the daily mean T, P, ET, and SM for each land surface model, and then the pentad-mean climatologies for each variable were computed. Second, the ensemble T, P, ET, and SM were computed based on three land surface models. Last, the ensemble P and SM were converted to percentiles using the time series values of P and SM in the period of 2000–2019. To evaluate the performance of land surface models, we calculated the frequency of occurrence (FOC) of each model. The FOC is defined as the percentage of pentads under flash droughts ($(N/N_{total})*100\%$) for each grid point. N_{total} represents the total number of pentads in the reference period, and N represents the number of pentads for the occurrence of flash droughts. Although the

magnitudes of the monthly-mean FOC from three land surface models are different, all the trends are similar for the period of 2000−2019 (Supplementary Fig. 11).

4.2 Definition of flash droughts

To robustly identify flash droughts, we took into account both the rapid intensification rate and the drought condition in this study: the pentad (5 days) indicates the root-zone SM decreasing from above the 40th percentile to below the 20th percentile, with an average decline rate of no less than the 5th percentile for each pentad. If the declining SM rises up to the 20th percentile again, flash droughts will terminate. In order to explore how fast flash drought evolves, we paid close attention to the onset development of flash droughts. As shown in Fig. 5, we calculated the decline rate in SM for the onset development period at each grid point. The onset point is defined as the first point where SM is over the 40th percentile and the decline begins at a rate greater than the 5th percentile. The end point of the onset development is defined as the first point where SM drops below the 20th percentile. Therefore, the onset development phase of flash droughts starts from the onset point (t_o) and terminates at the end point (t_e). The period from t_o to t_e is the timescale of the onset development phase, which is defined as the lead time of flash droughts. The whole duration of flash droughts begins from t_o to t_p. Specifically, the intensification rate and the drought condition are expressed in Equations (1) and (2), respectively.

$$Intensification\ rate: \begin{cases} \dfrac{SM(t_{i+1}) - SM(t_i)}{t_{i+1} - t_i} \geq 5th\ \ percentile \\ 0 < t_e - t_o \leq 5 \end{cases} \quad (1)$$

$$Drought\ condition: \begin{cases} SM(t_o) \geq 40th\ \ percentile \\ SM(t_e) \leq 20th\ \ percentile \\ t_p - t_e \geq 2 \end{cases} \quad (2)$$

To reach sufficient drought intensity and duration to largely diminish crop productivity and yield, SM should not only drop below the 20th percentile but also last for at least two pentads ($t_p - t_e \geq 2$). This criterion can also be used to exclude those events that decrease from above the 40th percentile to below the 20th percentile, and then recover up to the 40th percentile quickly (see Supplementary Fig. 12, many events experience such a rapid decrease but recover quickly, which should be excluded).

4.3 Detection of temporal trends

The Mann–Kendall (M-K) (Mann, 1945; Kendall, 1975) method is a nonparametric test, which is commonly used as the base method of trend detection to examine whether there is a monotonic trend in the time series of the variable of interest. In the M-K test, the null hypothesis, H_0, is that there is no monotonic trend in the series. The alternative hypothesis, H_1, is that the data has a monotonic trend (positive or negative). Positive values of standardized test statistic Z_{MK} indicate an increasing trend in the flash drought time series, whereas negative Z_{MK} values suggest a decreasing trend. The advantages of this method are that statistical analysis is not required and samples are not required to follow a certain distribution. Thus, this method is not affected by a few abnormal values, and can be used to well characterize the trend of a time series. The M-K trend

analysis was performed in this study to examine the trend of flash droughts on a global scale. For a given time series $(x_1, \ldots, x_n)$, the test statistic Z_{MK} was calculated as follows:

$$S = \sum_{i=1}^{n-1} \sum_{j=i+1}^{n} sign\left(x_j - x_i\right) \tag{3}$$

$$sign(x_j - x_i) = \begin{cases} +1, x_j > x_i \\ 0, \quad x_j = x_i \\ -1, x_j < x_i \end{cases} \tag{4}$$

$$Var(S) = \frac{1}{18}\left[n(n-1)(2n+5) - \sum_p t_p(t_p - 1)(2t_p + 5) \right] \tag{5}$$

$$Z_{MK} = \begin{cases} \dfrac{S-1}{\sqrt{Var(S)}} & if\ S > 0 \\ 0 & if\ S = 0 \\ \dfrac{S+1}{\sqrt{Var(S)}} & if\ S < 0 \end{cases} \tag{6}$$

where n is the length of the time series. x_i and x_j are sequential data in time series. t_p is the number of ties of the p_{th} value.

Data availability. All datasets are publicly available. The GLDAS-2 data can be downloaded from the Goddard Earth Sciences Data and Information Services Center (https://disc.sci.gsfc.nasa.gov/datasets?keywords=GLDAS). The pentad-mean soil moisture derived from three land surface models and the ensemble soil moisture can be accessed online (http://dx.doi.org/10.17632/4n8jcxy9sm.1). The data for the agriculture map of Supplementary Fig. 3 is available online (https://sedac.ciesin.columbia.edu/data/set/aglands-croplands-2000/data-download). For further requests, please contact the corresponding author.

Code availability. Statistical methods are illustrated in the Methods section of the paper. All analyzing data and drawing plots as well as computer codes are made using the open-source software R 4.0.2 and Python 3.8. Codes will be made available upon request.

Acknowledgments
This research was supported by the National Natural Science Foundation of China (Grant No. 51809223) and the Hong Kong Research Grants Council Early Career Scheme (Grant No. PP5Z).

Author contributions

Y.Q. and S.W. conceived the study and carried out the analysis. Y.Q. wrote the paper with contributions from all co-authors. B.C.A. and Z.L.Y. provided comments and suggestions for improving the quality of this study. The authors declare no conflict of interests.

References

Anderson, M. C., Hain, C., Otkin, J., Zhan, X., Mo, K., Svoboda, M., Wardlow, B., Pimstein, A. An intercomparison of drought indicators based on thermal remote sensing and NLDAS-2 simulations with U.S. Drought Monitor classifications. J. Hydrometeorol. 14 (4), 1035–1056 (2013). doi.org/10.1175/JHM-D-12-0140.1.

Anderson, M. C., Zolin, C. A., Sentelhas, P. C., Hain, C. R., Semmens, K., Tugrul Yilmaz, M., Gao F., Otkin, J. A., Tetrault, R. The evaporative stress index as an indicator of agricultural drought in Brazil: an assessment based on crop yield impacts. Remote. Sens. Environ. 174 82–99 (2016). doi.org/10.1016/j.rse.2015.11.034.

Barlage, M., Chen, F., Tewari, M., et al. Noah land surface model modifications to improve snowpack prediction in the Colorado Rocky Mountains. J. Geophys. Res. Atmos. 115, D22101 (2010). doi.org/10.1029/2009JD013470.

Basara, J. B., Christian, J. I., Wakefield, R. A., et al. The evolution, propagation, and spread of flash drought in the Central United States during. Environ. Res. Lett. 14 (8): 084025 (2019). doi.org/10.1088/1748-9326/ab2cc0.

Burrows, D. A., Ferguson, C. R., Campbell, M. A., et al. An objective classification and analysis of upper-level coupling to the Great Plains low-level jet over the twentieth century. J. Clim. 32 (21): 7127-7152 (2019). doi.org/10.1175/JCLI-D-18-0891.1.

Cheng, S., Guan, X., Huang, J., Ji, F., Guo, R. Long-term trend and variability of soil moisture over East Asia. J. Geophys. Res. Atmos. 120, 8658–8670 (2015). doi.org/10.1002/2015JD023206.

Christian, J. I., Basara, J. B., Hunt, E. D., et al. Flash drought development and cascading impacts associated with the 2010 Russian heatwave. Environ. Res. Let. 15 (9): 094078 (2020). doi.org/10.1088/1748-9326/ab9faf.

Christian, J. I., Basara, J. B., Otkin, J. A., et al. A methodology for flash drought identification: Application of flash drought frequency across the United States. J. Hydrometeorol. 20 (5): 833-846 (2019). doi.org/10.1175/JHM-D-18-0198.1.

Crausbay, S. D., Ramirez, A. R., Carter, S. L., et al. Defining Ecological Drought for the Twenty-First Century. Bull. Amer. Meteor. Soc. 98, 2543–2550 (2017). doi.org/10.1175/BAMS-D-16-0292.1.

Deng, A., Stauffer, D. R. On improving 4-km mesoscale model simulations. J. Appl. Meteorol. Climatol. 45 (3), 361–381 (2006). doi:10.1175/JAM2341.1.

Dorigo, W., de Jeu, R., Chung, D., Parinussa, R., Liu, Y., Wagner, W., Fernández-Prieto, D. Evaluating global trends (1988–2010) in harmonized multi-satellite surface soil moisture. Geophys. Res. Lett. 39, L18405 (2012). doi.org/10.1029/2012GL052988.

Ek, M. B., Mitchell, K. E., Lin, Y., Rogers, E., Grunmann, P., Koren, V., Gayno, G., Tarpley, J. D. Implementation of Noah land surface model advances in the National Centers for Environmental Prediction operational mesoscale Eta model. J. Geophys. Res. 108, 8851 (2003). doi.org/10.1029/2002JD003296.

Fischer, E. M., Seneviratne, S. I., Lüthi, D., et al. Contribution of land-atmosphere coupling to recent European summer heat waves. Geophys. Res. Lett. 34 (6) (2007). doi.org/10.1029/2006GL029068.

Ford, T. W., Labosier, C. F. Meteorological conditions associated with the onset of flash drought in the eastern United States. Agric. Forest. Meteorol. 247: 414-423, (2017). doi.org/10.1016/j.agrformet.2017.08.031.

Ford, T. W., McRoberts, D. B., Quiring, S. M., et al. On the utility of in situ soil moisture observations for flash drought early warning in Oklahoma. Geophys. Res. Lett. 42 (22): 9790-9798 (2015). doi.org/10.1002/2015GL066600.

Gerken, T., Bromley, G. T., Ruddell, B. L., et al. Convective suppression before and during the United States Northern Great Plains flash drought of 2017. Hydrol. Earth Syst. Sci. 22 (8) (2018). doi.org/10.5194/hess-22-4155-2018.

Hendon, H. H., et al. Australian rainfall and surface temperature variations associated with the Southern Hemisphere annular mode. J. Clim. 20, 2452–2467 (2007). doi.org/10.1175/JCLI4134.1.

Hobbins, M. T., Wood, A., Mcevoy, D. J., Huntington, J. L., Morton, C., Anderson, M., Hain, C. The evaporative demand drought index. Part I: linking drought evolution to variations in evaporative demand. J. Hydrometeor. 1745–61 (2016). doi.org/10.1175/JHM-D-15-0121.1.

Hoerling, M. P., et al. Causes and predictability of the 2012 Great Plains drought. Bull. Am. Meteor. Soc. 95, 269–282 (2014). doi.org/10.1175/BAMS-D-13-00055.1.

Hoerling, M., Eischeid, J., Kumar, A., Leung, R., Mariotti, A., Mo, K., Schubert, S., Seager, R. Causes and Predictability of the 2012 Great Plains Drought. Bull. Amer. Meteor. Soc. 95, 269–282 (2014). doi.org/10.1175/BAMS-D-13-00055.1.

Huang, R., Chen, J., Huang, G. Characteristics and variations of the East Asian monsoon system and its impacts on climate disasters in China. Adv. Atmos. Sci. 24, 993–1023 (2007). doi.org/10.1007/s00376-007-0993-x.

Hunt, E. D., Hubbard, K. G., Wilhite, D. A., Arkebauer, T. J., Dutcher, A. L. The development and evaluation of a soil moisture index. Int. J. Clim. 29(5), 747–759 (2009). doi.org/10.1002/joc.1749.

Hunt, E. D., Svoboda, M., Wardlow, B., Hubbard, K., Hayes, M., Arkebauer, T. Monitoring the effects of rapid onset of drought on non-irrigated Maize with agronomic data and climate-based drought indices. Agric. Forest. Meteorol. 191 1–11 (2014). doi.org/10.1016/j.agrformet.2014.02.001.

Jia, B., Liu, J., Xie, Z., Shi, C. Interannual variations and trends in remotely sensed and modeled soil moisture in China. J. Hydrometeor. 19 (5), 831–847 (2018). doi.org/10.1175/JHM-D-18-0003.1.

Jin, C., Luo, X., Xiao, X. et al. The 2012 Flash Drought Threatened US Midwest Agroecosystems. Chin. Geogr. Sci. 29, 768–783 (2019). doi.org/10.1007/s11769-019-1066-7

Jun, L., Zhaoli, W., Xushu, W., Shenglian, G., Xiaohong, C. Flash droughts in the Pearl River Basin, China: Observed characteristics and future changes. Sci. Total. Environ. (2020). doi.org/10.1016/j.scitotenv.2019.136074.

Koster, R. D., Schubert, S. D., Suarez, M. Analyzing the concurrence of meteorological droughts and warm periods, with implications for the determination of evaporative regime. J. Climate 22, 3331–3341 (2009). doi:10.1175/2008JCLI2718.1.

Kumar, S., Newman, M., Lawrence, D. M., et al. The GLACE-Hydrology Experiment: Effects of Land–Atmosphere Coupling on Soil Moisture Variability and Predictability. J. Clim. 33 (15): 6511-6529 (2020). doi.org/10.1175/JCLI-D-19-0598.1.

Lau, K. M., Yang, S. Climatology and interannual variability of the Southeast Asian summer monsoon. Adv. Atmos. Sci. 14, 141–162 (1997). doi.org/10.1007/s00376-997-0016-y.

Liang, X., Wood, E. F., Lettenmaier, D. P. Surface and soil moisture parameterization of the VIC-2L model: Evaluation and modifications. Global Planet. Change 13, 195–206 (1996). doi.org/10.1016/0921-8181(95)00046-1.

Liu, Y., Zhu, Y., Ren, L., Otkin, J., Hunt, E. D., Yang, X., Yuan, F., Jiang, S. Two Different Methods for Flash Drought Identification: Comparison of Their Strengths and Limitations. J. Hydrometeor. 21, 691–704 (2020). doi.org/10.1175/JHM-D-19-0088.1.

Liu, Y., Zhu, Y., Zhang, L., Ren, L., Yuan, F., Yang, X., Jiang, S. Flash droughts characterization over China: From a perspective of the rapid intensification rate. Sci. Total Environ. 704, 135373 (2020). doi.org/10.1016/J.SCITOTENV.2019.135373.

Lorenz, D. J., Otkin, J. A., Svoboda, M., et al. Forecasting rapid drought intensification using the Climate Forecast System (CFS). J. Geophys. Res. Atmos. 123(16): 8365-8373 (2018). doi.org/10.1029/2018JD028880.

Mahto, S. S., Mishra, V. Dominance of summer monsoon flash droughts in India. Environ. Res. Lett. 15 (10): 104061 (2020). doi.org/10.1088/1748-9326/abaf1d.

Mcevoy, D. J., Huntington, J. L., Hobbins, M. T., Wood, A., Morton, C., Anderson, M., Hain, C. The evaporative demand drought index. Part II: CONUS-wide assessment against common drought indicators. J. Hydrometeor. 17 1763–1779 (2016). doi.org/10.1175/JHM-D-15-0122.1.

Mo, K. C., Lettenmaier, D. P. Precipitation deficit flash droughts over the United States. J. Hydrometeor. 17 (4): 1169-1184 (2016). doi.org/10.1175/JHM-D-15-0158.1.

Mozny, M., Trnka, M., Zalud, Z., Hlavinka, P., Nekovar, J., Potop, V., Virag, M. Use of a soil moisture network for drought monitoring in the Czech Republic. Theor. Appl. Climatol. 107 (1–2), 99–111 (2012). doi.org/10.1007/s00704-011-0460-6.

Namias, J. Some causes of United States drought. J. Climate Appl. Meteor. 22 (1): 30-39 (1983). http://www.jstor.org/stable/26180894.

Nguyen, H., et al. Using the evaporative stress index to monitor flash drought in Australia. Environ. Res. Let. (2019). doi.org/10.1088/1748-9326/ab2103.

Osman, M., Zaitchik, B. F., Badr, H. S., et al. Flash drought onset over the Contiguous United States: Sensitivity of inventories and trends to quantitative definitions. Hydrol. Earth Syst. Sci. 25 (2): 565–581 (2021). doi.org/10.5194/hess-25-565-2021.

Otkin, J. A., Anderson, M. C., Hain, C., et al. Using temporal changes in drought indices to generate probabilistic drought intensification forecasts. J. Hydrometeor. 16 (1): 88-105 (2015a). doi.org/10.1175/JHM-D-14-0064.1.

Otkin, J. A., Anderson, M. C., Hain, C., Svoboda, M., Johnson, D., Mueller, R., Tadesse, T., Wardlow, B., Brown, J. Assessing the evolution of soil moisture and vegetation conditions during the 2012 United States flash drought. Agric. Forest. Meteorol. 218–219, 230–42 (2016). doi.org/10.1016/j.agrformet.2015.12.065.

Otkin, J. A. et al. Flash droughts: a review and assessment of the challenges imposed by rapid-onset droughts in the United States. Bull. Am. Meteor. Soc. 99, 911–919 (2018). doi.org/10.1175/BAMS-D-17-0149.1.

Otkin, J. A., Anderson, M. C., Hain, C., Svoboda, M. Examining the relationship between drought development and rapid changes in evaporative stress index. J. Hydrometeorol. 15 (3), 938–956 (2014). doi.org/10.1175/JHM-D-13-0110.1.

Otkin, J. A., Shafer, M., Svoboda, M., Wardlow, B., Anderson, M. C., Hain, C., Basara, J. Facilitating the use of drought early warning information through interactions with agricultural stakeholders. Bull. Amer. Meteor. Soc. 96, 1073-1078 (2015b). doi.org/10.1175/BAMS-D-14-00219.1.

Pendergrass, A. G., Meehl, G. A., Pulwarty, R. et al. Flash droughts present a new challenge for subseasonal-to-seasonal prediction. Nat. Clim. Change 10, 191–199 (2020). doi.org/10.1038/s41558-020-0709-0.

Rajib, K., Indranil, D., Debashis, D., Amitava, R. Potential Effects of Climate Change on Soil Properties: A Review. Sci. International. 4: 51-73 (2016). doi.org/10.17311/sciintl.2016.51.73.

Rienecker, M. M. et al. MERRA: NASA's Modern-Era Retrospective Analysis for Research and Applications. J. Climate 24, 3624–3648 (2011). doi.org/10.1175/JCLI-D-11-00015.1.

Schubert, S., Gutzler, D., Wang, H., et al. A U.S. CLIVAR project to assess and compare the responses of global climate models to drought-related SST forcing patterns: Overview and results. J. Clim. 22 (19): 5251-5272 (2009). doi.org/10.1175/2009JCLI3060.1.

Sivakumar, B. Global climate change and its impacts on water resources planning and management: assessment and challenges. Stoch. Environ. Res. Risk. Assess. 25, 583–600 (2011). doi.org/10.1007/s00477-010-0423-y.

Soares, P. M. M., Careto, J. A. M., Cardoso, R. M., et al. Land-atmosphere coupling regimes in a future climate in Africa: From model evaluation to projections based on CORDEX-Africa. J. Geophys. Res. Atmos. 124 (21): 11118-11142 (2019). doi.org/10.1029/2018JD029473.

Sun, Y., Fu, R., Dickinson, R., Joiner, J., Frankenberg, C., Gu, L., Xia, Y., Fernando, N. Drought onset mechanisms revealed by satellite solar-induced chlorophyll fluorescence: insights from two contrasting extreme events. J. Geophys. Res. Biogeosci. 120 2427–40 (2015). doi.org/10.1002/2015JG003150.

571 Svoboda, M., et al. The Drought Monitor. Bull. Am. Meteorol. Soc. 83, 1181–1190 (2002).
572 doi.org/10.1175/1520-0477-83.8.1181.

573 Thacker, M. T. F., Lee, R., Sabogal, R. I., Henderson, A. Overview of deaths associated with
574 natural events, United States, 1979–2004. Disasters 32, 303–315 (2008).
575 doi.org/10.1111/j.1467-7717.2008.01041.x.

576 Waliser, D. E., et al. Potential predictability of the Madden–Julian oscillation. Bull. Am. Meteorol.
577 Soc. 84, 33–50 (2003). doi.org/10.1175/BAMS-84-1-33.

578 Wang, L., Yuan, X. Two Types of Flash Drought and Their Connections with Seasonal Drought.
579 Adv. Atmos. Sci. 35, 1478–1490 (2018). doi.org/10.1007/s00376-018-8047-0.

580 Wang, L., Yuan, X., Xie, Z., Wu, P., Li, Y. Increasing flash droughts over China during the recent
581 global warming hiatus. Sci. Rep. 6, 30571 (2016). doi.org/10.1038/srep30571.

582 Wei, H., Xia, Y., Mitchell, K. E., Ek, M. B. Improvement of the Noah land surface model for warm
583 season processes: Evaluation of water and energy flux simulation. Hydrol. Processes. 27,
584 297–303 (2013). doi.org/10.1002/hyp.9214.

585 Wen, L., Zhao, K., Zhang, G., et al. Statistical characteristics of raindrop size distributions
586 observed in East China during the Asian summer monsoon season using 2-D video
587 disdrometer and Micro Rain Radar data. J. Geophys. Res. Atmos. 121 (5): 2265-2282
588 (2016). doi.org/10.1002/2015JD024160.

589 Xia, Y., Mitchell, K., Ek, M., et al. Continental-scale water and energy flux analysis and validation
590 of the North American Land Data Assimilation System project phase 2 (NLDAS-2): 1.
591 Intercomparison and application of model products. J. Geophys. Res. 117, D03109
592 (2012a). doi.org/10.1029/2011JD016048.

593 Xia, Y., Ek, M. B., Wei, H., Meng, J. Comparative analysis of relationships between NLDAS-2
594 forcings and model outputs. Hydrol. Processes. 26, 467–474 (2012b).
595 doi.org/10.1002/hyp.8240.

596 Yang, H. B., Yang, D. W. Climatic factors influencing changing pan evaporation across China
597 from 1961 to 2001. J. Hydrol. 414–415, pp. 184-193 (2012).
598 doi.org/10.1016/j.jhydrol.2011.10.043.

599 Yuan, X., Ma, Z., Pan, M., Shi, C. Microwave remote sensing of short-term droughts during crop
600 growing seasons. Geophys. Res. Lett. 42, 4394–4401 (2015).
601 doi.org/10.1002/2015GL064125.

602 Yuan, X., Wang, L., Wu, P., et al. Anthropogenic shift towards higher risk of flash drought over
603 China. Nat. Commun. 10 (1): 1–8 (2019). doi.org/10.1038/s41467-019-12692-7.

604 Yuan, X., Wang, L. Y., Wood, E. F. Anthropogenic intensification of southern African flash
605 droughts as exemplified by the 2015/16 season. Bull. Am. Meteor. Soc., 99, S86–S90
606 (2018). doi.org/10.1175/BAMS-D-17-0077.1.

607 Zawadzki, J., Kedzior, M. A. Statistical analysis of soil moisture content changes in Central
608 Europe using GLDAS database over three past decades. Cent. Eur. J. Geo. 6 (3), 344–353
609 (2014). doi.org/10.2478/s13533-012-0176-x.

Zhang, M., He, J., Wang, B., et al. Extreme drought changes in Southwest China from 1960 to 2009. J. Geogr. Sci. 23, 3–16 (2013). doi.org/10.1007/s11442-013-0989-7.

Zhang, R. H., Sumi, A., Kimoto, M. Impact of El Niño the East Asian monsoon: A diagnostic study of the 86/87 and 91/92 events. J. Meteor. Soc. Japan 74, 49–62 (1996). doi.org/10.2151/jmsj1965.74.1_49.

Zhang, Y., You. Q., Chen. C., et al. Flash droughts in a typical humid and subtropical basin: A case study in the Gan River Basin, China. J. Hydrol. 551: 162–176 (2017). doi.org/10.1016/j.jhydrol.2017.05.044.

List of Figure Captions

Fig. 1 Comparison of variations in soil moisture percentiles, mean frequencies, and mean durations of flash droughts based on new and old definitions. **a**, **b** Temporal variations in soil moisture (SM) percentiles for flash drought events of all grid points. **c**, **d** The mean frequencies of flash droughts. **e**, **f** The mean durations (pentads) of flash droughts. New: SM decreases from above the 40th percentile to below the 20th percentile with an average decline rate of no less than the 5th percentile for each pentad, and the SM below the 20th percentile should last for no less than 2 pentads. If the declining soil moisture rises up to the 20th percentile, flash droughts will terminate. Old: The pentad-mean surface temperature (T) anomaly > one standard deviation, ET anomaly > 0, and SM percentile < 40% for heat wave flash droughts. The pentad-mean surface temperature (T) anomaly > one standard deviation, ET anomaly < 0, and precipitation (P) < 40% for precipitation deficit flash droughts. **d** The total number of heat wave flash droughts and precipitation deficit flash droughts. **f** The mean duration of heat wave flash droughts and precipitation deficit flash droughts.

Fig. 2 The percentage of flash droughts at different lead times among all flash droughts and the onset development mean intensification rate of flash droughts at different lead times. **a** The regional proportion of flash droughts that last for different pentads among all flash droughts as well as their mean intensification rates. **b** as in **a**, but for the global.

Fig. 3 The Mann-Kendall trends in the percentages of flash droughts at different lead times among all flash droughts. Trends that are statistically significant at the 90% level are highlighted by the black dashed line on maps. **a-c** Spatial distributions of trends in the percentages of flash droughts that last for less than or equal to 3 pentads as well as 4 and 5 pentads among all flash droughts. **d-f** Percentages of areas with downward and upward trends based on **a-c**.

Fig. 4 a-c Temporal evolution of the percentages of flash droughts that last for less than or equal to 3 pentads as well as 4 and 5 pentads among all flash droughts. **d** Temporal evolution of the onset development mean intensification rate of flash droughts. **e** Temporal evolution of the percentages of flash droughts among all droughts. **f** Spatial distributions of the percentages of flash droughts among all drought events. The grey shadows are the ranges of results derived from different land surface models, and the red dashed lines in **a-e** are the trends in temporal evolution.

Fig. 5 a Schematic representation of the method used to identify flash droughts. Soil moisture (SM) decreases from above the 40th percentile to below the 20th percentile with an average decline rate of no less than the 5th percentile for each pentad, and SM below the 20th percentile should last for no less than 2 pentads. The blue solid line represents the 5-day mean SM percentile for a grid point. The two black dashed lines represent the wet (high SM percentile) and the dry (low SM percentile) conditions of SM, respectively. The purple shaded area represents the onset development of flash droughts. **b** Illustration of the onset development phase of flash droughts. MIR in **b** denotes the mean intensification rate of the onset development phase, which is defined as Intensification/Timescale.

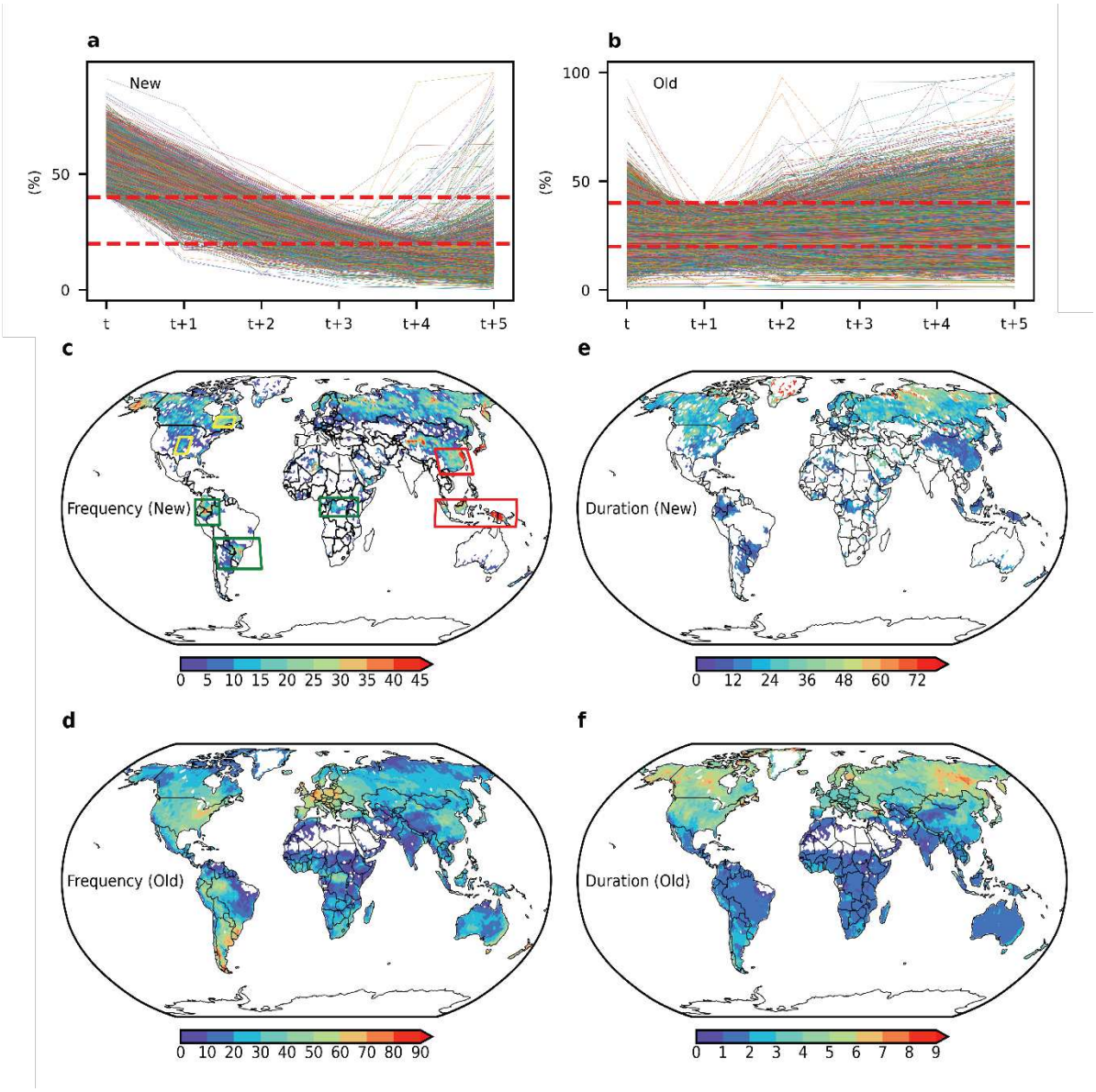

Fig. 1 Comparison of variations in soil moisture percentiles, mean frequencies, and mean durations of flash droughts based on new and old definitions. **a**, **b** Temporal variations in soil moisture (SM) percentiles for flash drought events of all grid points. **c**, **d** The mean frequencies of flash droughts. **e**, **f** The mean durations (pentads) of flash droughts. New: SM decreases from above the 40th percentile to below the 20th percentile with an average decline rate of no less than the 5th percentile for each pentad, and the SM below the 20th percentile should last for no less than 2 pentads. If the declining soil moisture rises up to the 20th percentile, flash droughts will terminate. Old: The pentad-mean surface temperature (T) anomaly > one standard deviation, ET anomaly > 0, and SM percentile < 40% for heat wave flash droughts. The pentad-mean surface temperature (T) anomaly > one standard deviation, ET anomaly < 0, and precipitation (P) < 40% for precipitation deficit flash droughts. **d** The total number of heat wave flash droughts and precipitation deficit flash droughts. **f** The mean duration of heat wave flash droughts and precipitation deficit flash droughts.

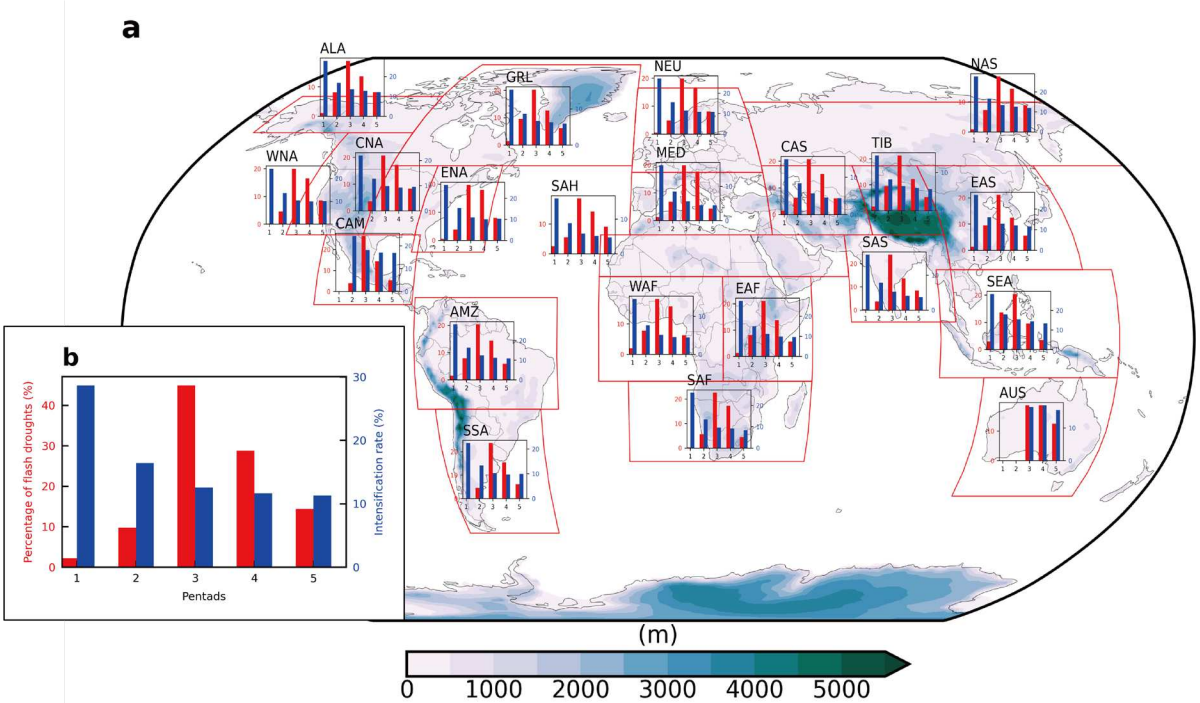

673

674 **Fig. 2** The percentage of flash droughts at different lead times among all flash droughts and the onset
675 development mean intensification rate of flash droughts at different lead times. **a** The regional proportion
676 of flash droughts that last for different pentads among all flash droughts as well as their mean intensification
677 rates. **b** as in **a**, but for the global.

678

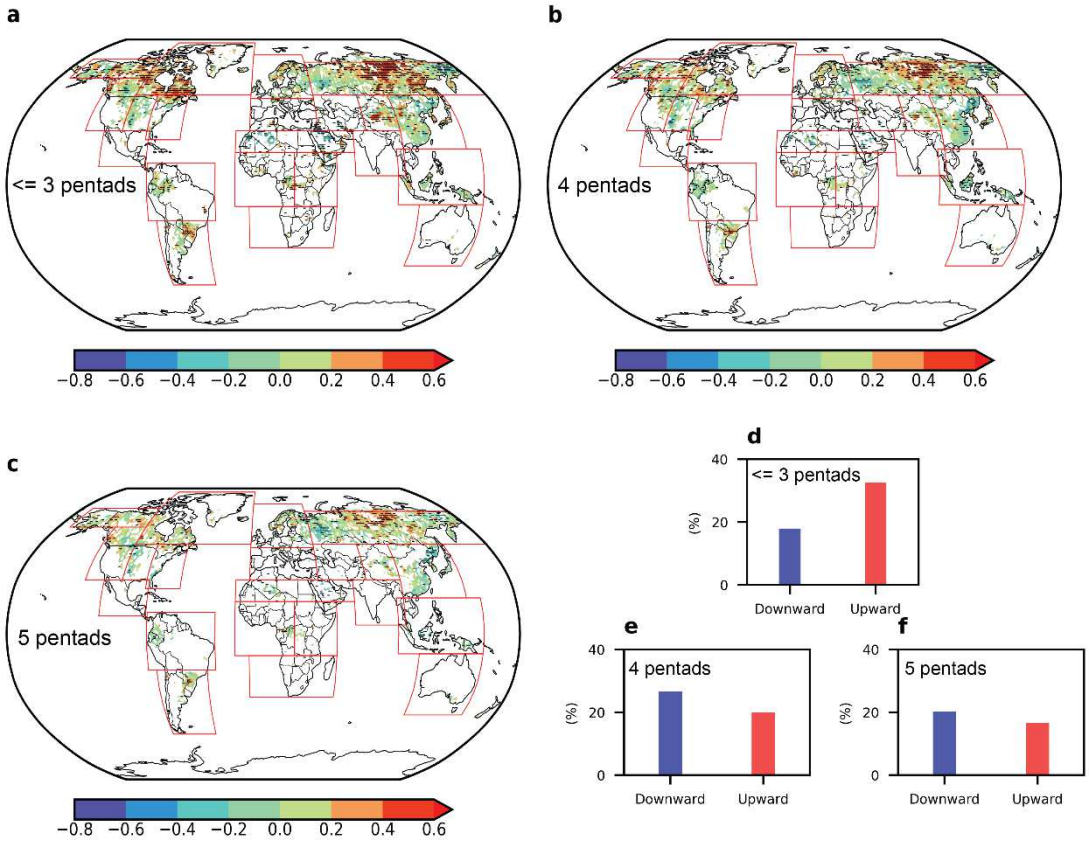

679

680

681 **Fig. 3** The Mann-Kendall trends in the percentages of flash droughts at different lead times among all flash
682 droughts. Trends that are statistically significant at the 90% level are highlighted by the black dashed line
683 on maps. **a-c** Spatial distributions of trends in the percentages of flash droughts that last for less than or
684 equal to 3 pentads as well as 4 and 5 pentads among all flash droughts. **d-f** Percentages of areas with
685 downward and upward trends based on **a-c**.

686

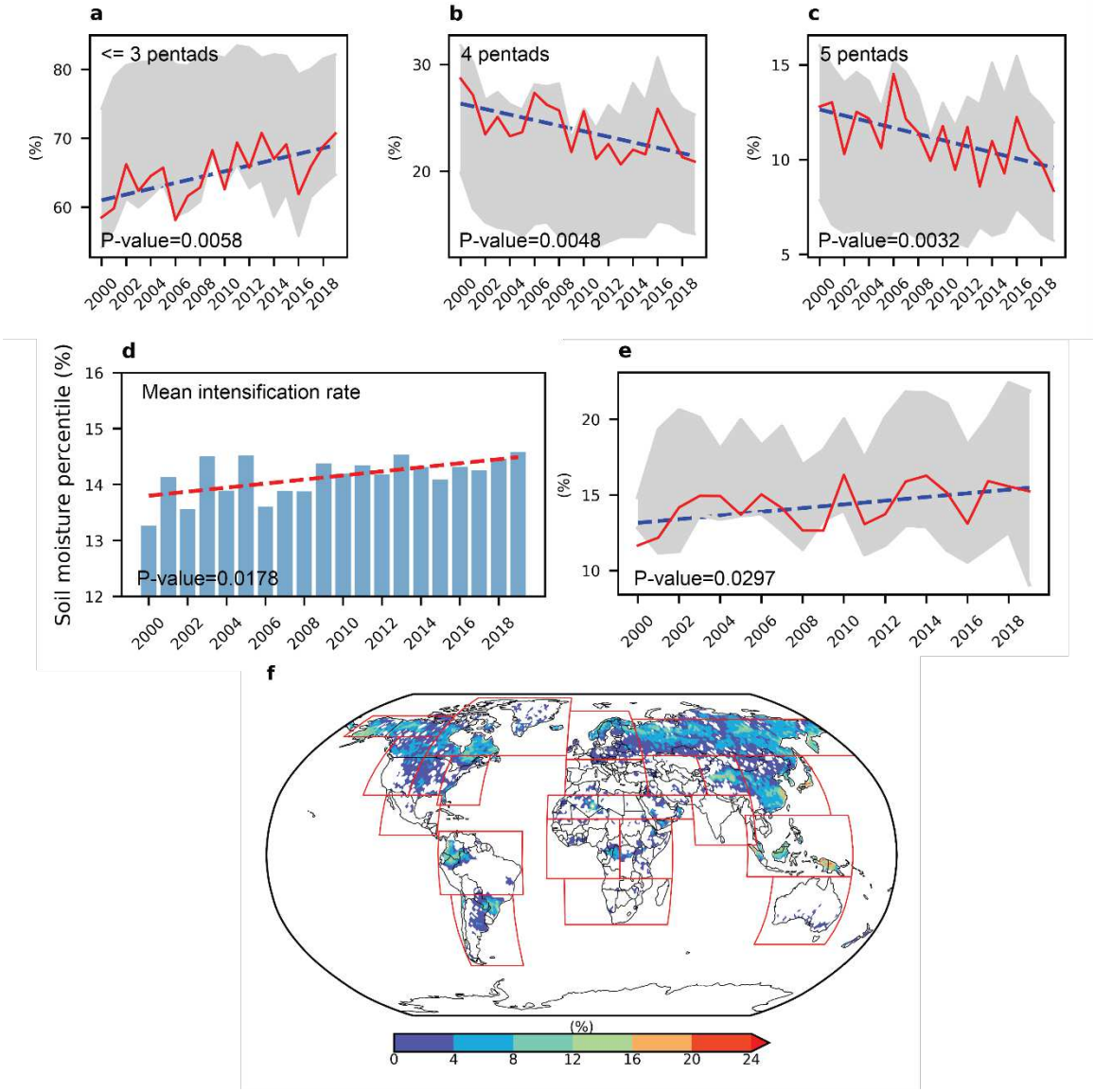

687

688 **Fig. 4 a-c** Temporal evolution of the percentages of flash droughts that last for less than or equal to 3
689 pentads as well as 4 and 5 pentads among all flash droughts. **d** Temporal evolution of the onset development
690 mean intensification rate of flash droughts. **e** Temporal evolution of the percentages of flash droughts
691 among all droughts. **f** Spatial distributions of the percentages of flash droughts among all drought events.
692 The grey shadows are the ranges of results derived from different land surface models, and the red dashed
693 lines in **a-e** are the trends in temporal evolution.

694

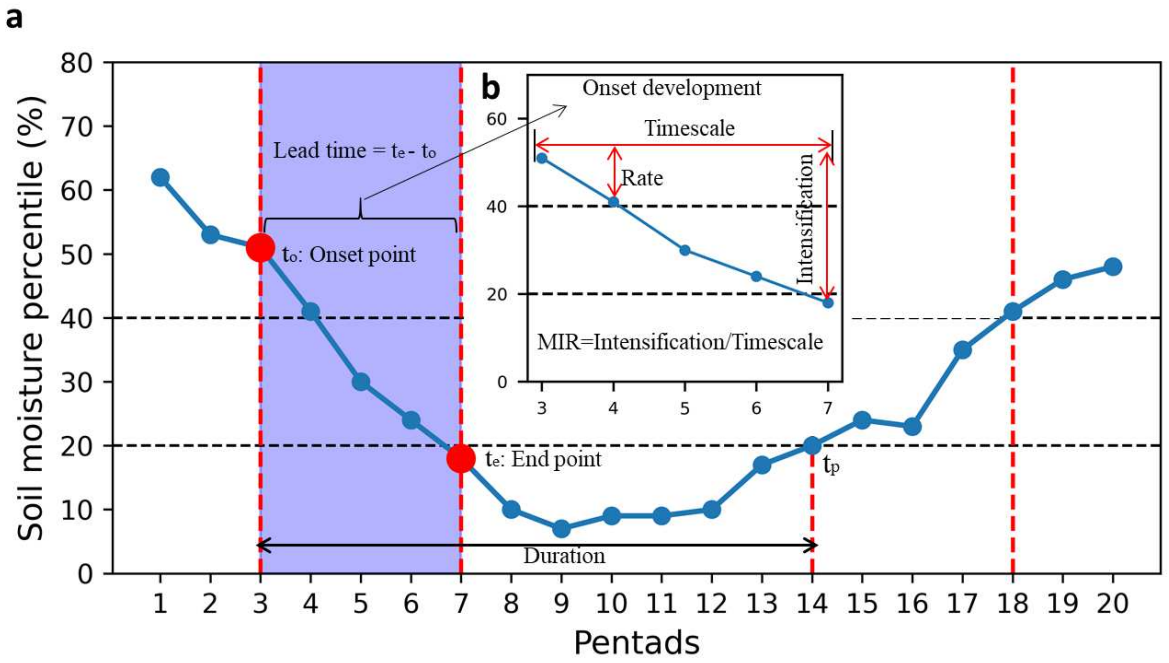

Fig. 5 a Schematic representation of the method used to identify flash droughts. Soil moisture (SM) decreases from above the 40th percentile to below the 20th percentile with an average decline rate of no less than the 5th percentile for each pentad, and SM below the 20th percentile should last for no less than 2 pentads. The blue solid line represents the 5-day mean SM percentile for a grid point. The two black dashed lines represent the wet (high SM percentile) and the dry (low SM percentile) conditions of SM, respectively. The purple shaded area represents the onset development of flash droughts. **b** Illustration of the onset development phase of flash droughts. MIR in **b** denotes the mean intensification rate of the onset development phase, which is defined as Intensification/Timescale.

Figures

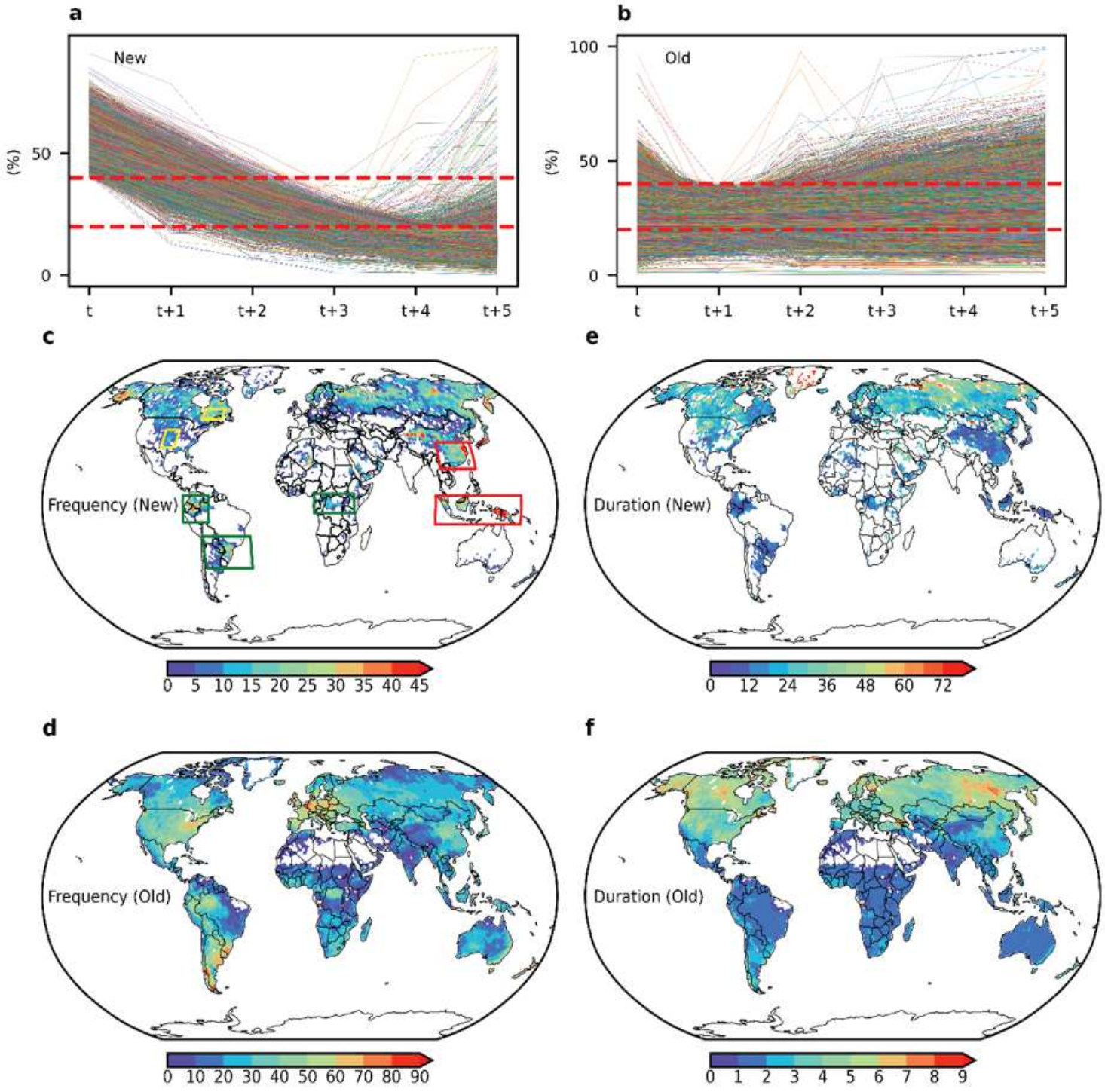

Figure 1

Comparison of variations in soil moisture percentiles, mean frequencies, and mean durations of flash droughts based on new and old definitions. a, b Temporal variations in soil moisture (SM) percentiles for flash drought events of all grid points. c, d The mean frequencies of flash droughts. e, f The mean durations (pentads) of flash droughts. New: SM decreases from above the 40th percentile to below the

20th percentile with an average decline rate of no less than the 5th percentile for each pentad, and the SM below the 20th percentile should last for no less than 2 pentads. If the declining soil moisture rises up to the 20th percentile, flash droughts will terminate. Old: The pentad-mean surface temperature (T) anomaly > one standard deviation, ET anomaly > 0, and SM percentile < 40% for heat wave flash droughts. The pentad-mean surface temperature (T) anomaly > one standard deviation, ET anomaly < 0, and precipitation (P) < 40% for precipitation deficit flash droughts. d The total number of heat wave flash droughts and precipitation deficit flash droughts. f The mean duration of heat wave flash droughts and precipitation deficit flash droughts. Note: The designations employed and the presentation of the material on this map do not imply the expression of any opinion whatsoever on the part of Research Square concerning the legal status of any country, territory, city or area or of its authorities, or concerning the delimitation of its frontiers or boundaries. This map has been provided by the authors.

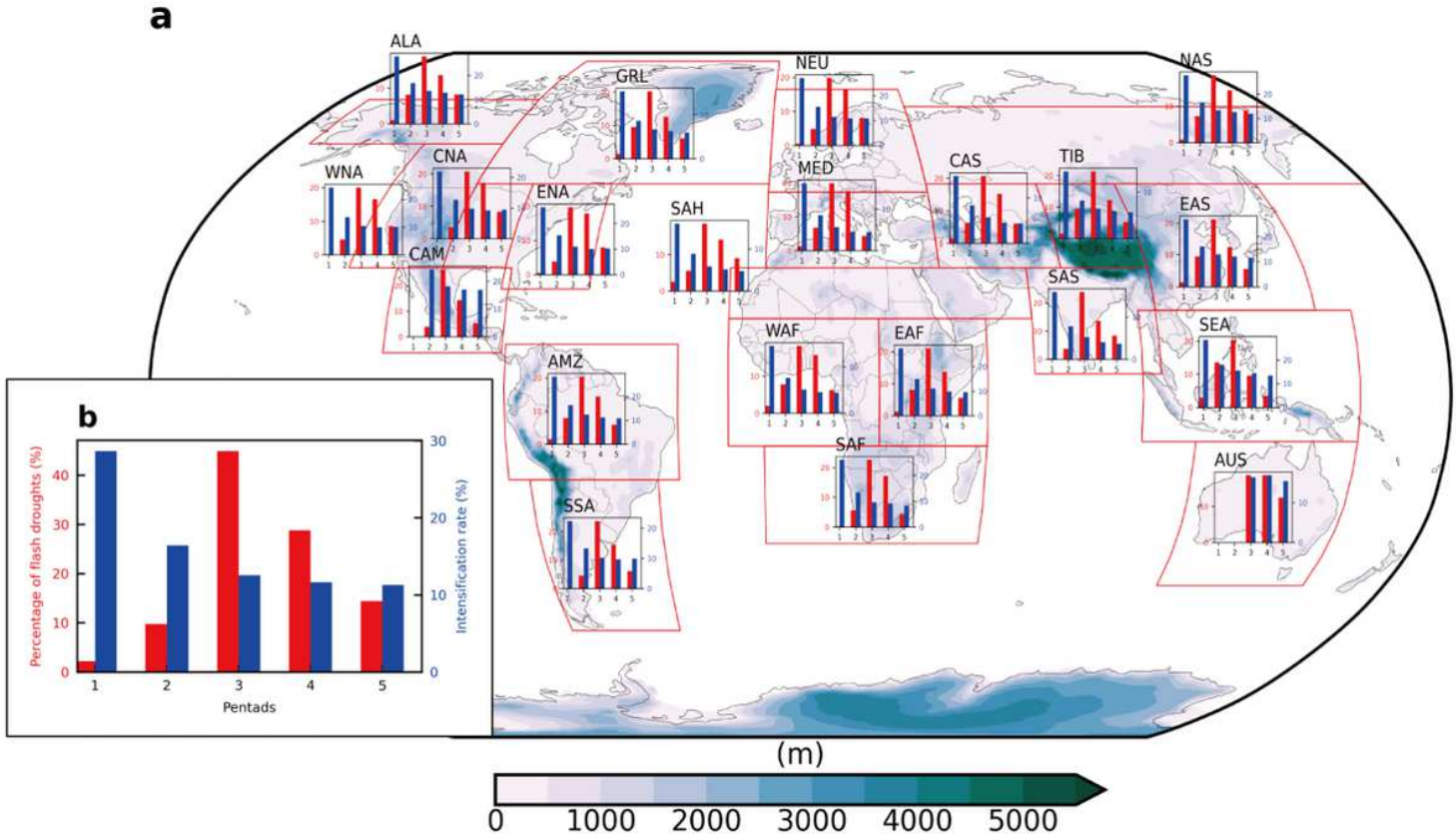

Figure 2

The percentage of flash droughts at different lead times among all flash droughts and the onset development mean intensification rate of flash droughts at different lead times. a The regional proportion of flash droughts that last for different pentads among all flash droughts as well as their mean intensification rates. b as in a, but for the global. Note: The designations employed and the presentation of the material on this map do not imply the expression of any opinion whatsoever on the part of Research Square concerning the legal status of any country, territory, city or area or of its authorities, or concerning the delimitation of its frontiers or boundaries. This map has been provided by the authors.

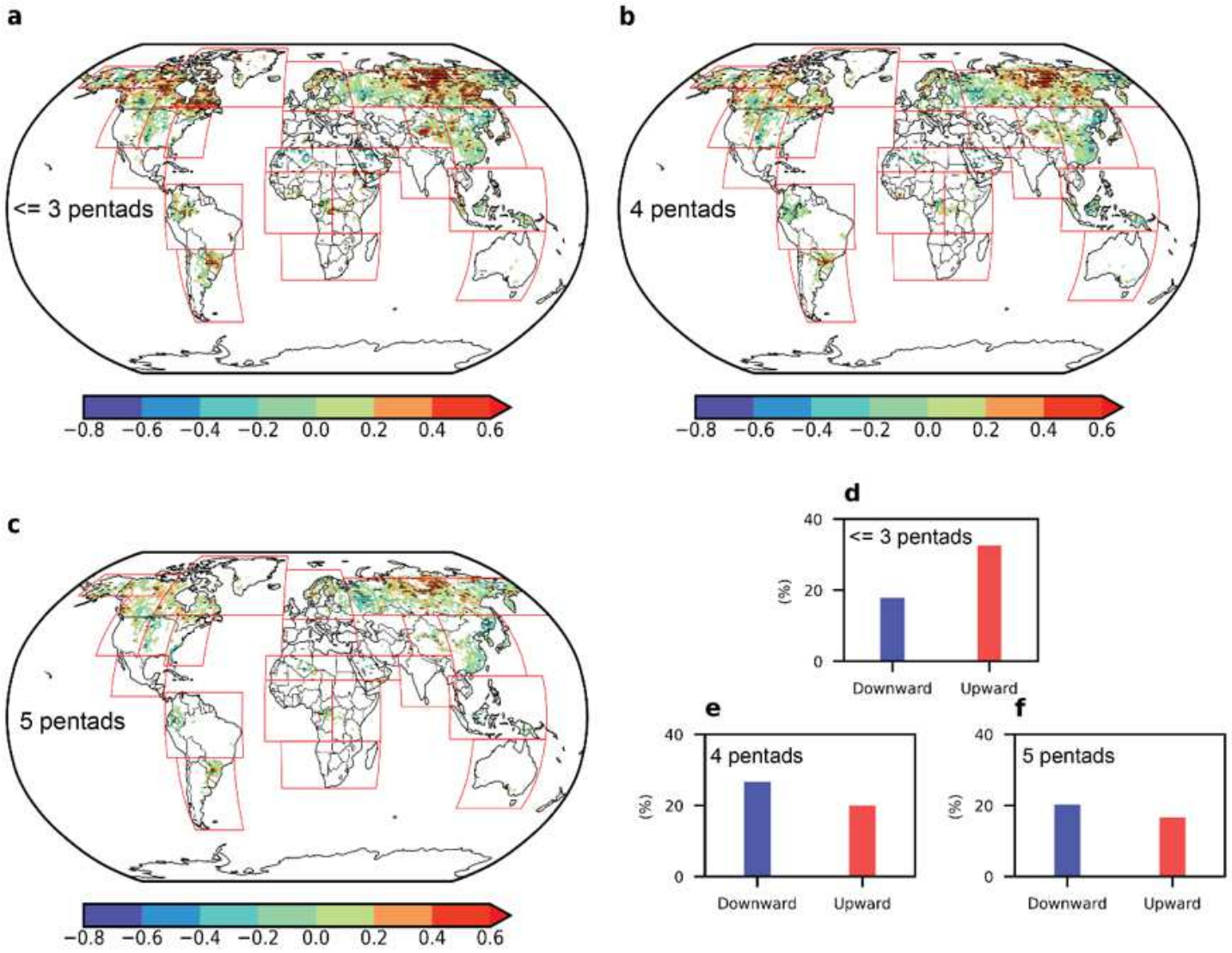

Figure 3

The Mann-Kendall trends in the percentages of flash droughts at different lead times among all flash droughts. Trends that are statistically significant at the 90% level are highlighted by the black dashed line on maps. a-c Spatial distributions of trends in the percentages of flash droughts that last for less than or equal to 3 pentads as well as 4 and 5 pentads among all flash droughts. d-f Percentages of areas with downward and upward trends based on a-c. Note: The designations employed and the presentation of the material on this map do not imply the expression of any opinion whatsoever on the part of Research Square concerning the legal status of any country, territory, city or area or of its authorities, or concerning the delimitation of its frontiers or boundaries. This map has been provided by the authors.

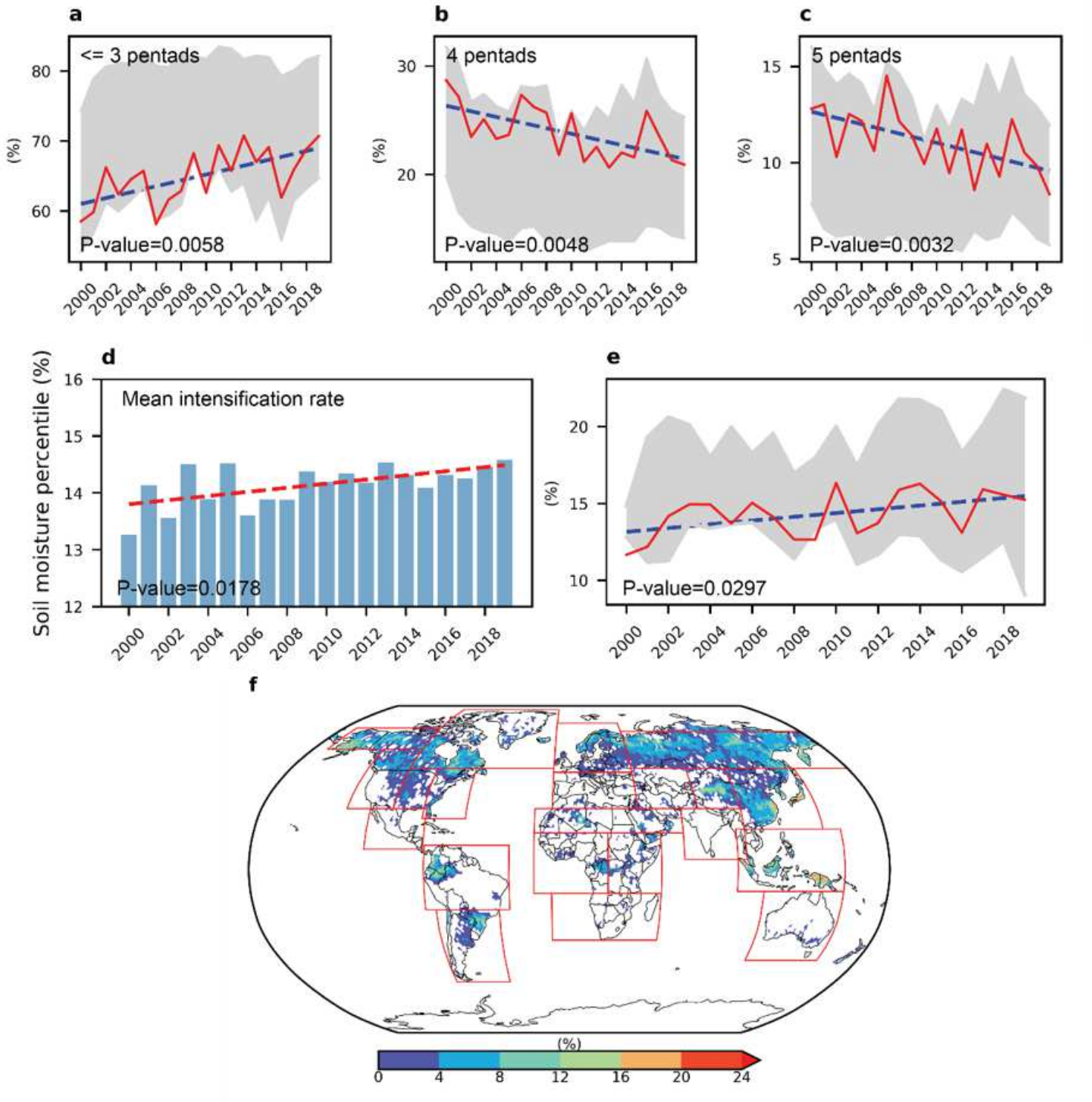

Figure 4

a-c Temporal evolution of the percentages of flash droughts that last for less than or equal to 3 pentads as well as 4 and 5 pentads among all flash droughts. d Temporal evolution of the onset development mean intensification rate of flash droughts. e Temporal evolution of the percentages of flash droughts among all droughts. f Spatial distributions of the percentages of flash droughts among all drought events. The grey shadows are the ranges of results derived from different land surface models, and the red dashed lines in a-e are the trends in temporal evolution. Note: The designations employed and the

presentation of the material on this map do not imply the expression of any opinion whatsoever on the part of Research Square concerning the legal status of any country, territory, city or area or of its authorities, or concerning the delimitation of its frontiers or boundaries. This map has been provided by the authors.

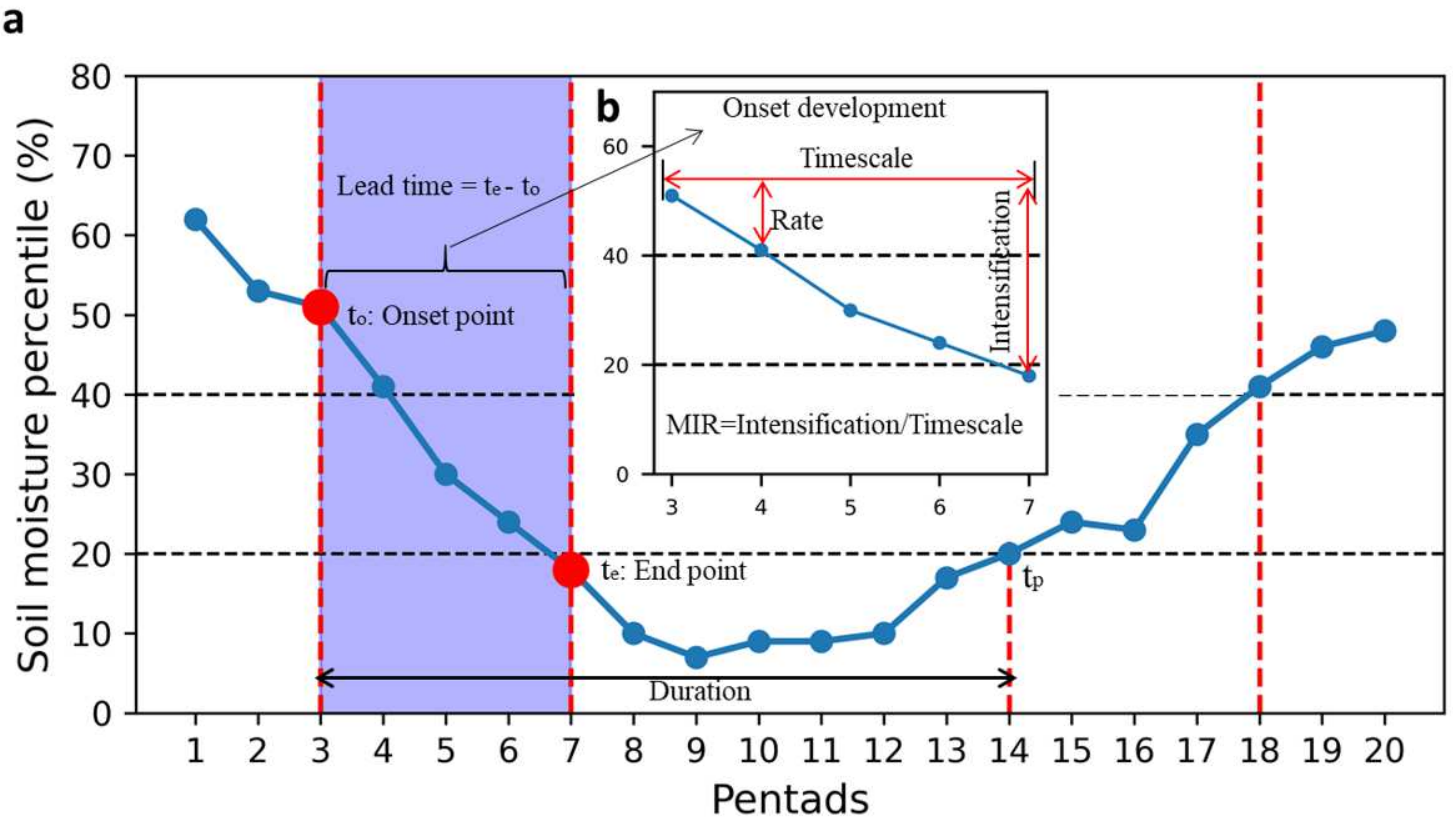

Figure 5

a Schematic representation of the method used to identify flash droughts. Soil moisture (SM) decreases from above the 40th percentile to below the 20th percentile with an average decline rate of no less than the 5th percentile for each pentad, and SM below the 20th percentile should last for no less than 2 pentads. The blue solid line represents the 5-day mean SM percentile for a grid point. The two black dashed lines represent the wet (high SM percentile) and the dry (low SM percentile) conditions of SM, respectively. The purple shaded area represents the onset development of flash droughts. b Illustration of the onset development phase of flash droughts. MIR in b denotes the mean intensification rate of the onset development phase, which is defined as Intensification/Timescale.

Supplementary Files

This is a list of supplementary files associated with this preprint. Click to download.

- SupplementaryMaterial.docx